Journal of Applied Polymer Science

Micro-Gels for Impact Protection

Chao Zhou,[1] Bo Wang,[2] Fengtao Zhang,[1] Kun Xu,[2] Changyu Han,[2] Hong Hu,[3] Yanpin Liu,[3] Pixin Wang,[2] John H. Xin[3]

[1]Changchun University of Technology, College of Chemistry and Chemical Engineering, Changchun 130012, China
[2]Key Laboratory of Polymer Ecomaterials, Changchun Institute of Applied Chemistry, Chinese Academy of Sciences, Changchun 130022, China
[3]Institute of Textile and Clothing, The Hong Kong Polytechnic University, Hung Hom, Hong Kong
Correspondence to: H. Hu (E-mail: tchuhong@polyu.edu.hk); K. Xu (E-mail: xukun@ciac.jl.cn)

ABSTRACT: A novel kind of impact protective material, named as impact protective micro-gel (IPM), was synthesized via a precipitation copolymerization of a compound containing boron and silanol. Diphenylmethane diisocyanate (MDI) was introduced as the chain extender to enhance its impact protective performance. Its rheological properties and morphology were investigated. Three-dimensional (3D) spacer warp-knitted fabrics were dip-coated with the IPM made with and without use of MDI, and the impact protective performance of 3D finished fabrics was assessed by drop impact tests. The results show that the adjustment of the MDI content can adjust the real cross-linking density of the IPM due to the entanglement of polymer chains, and an appropriate cross-linking density can endow dilatant properties to the IPM samples. The results also show that the impact protective performance of 3D spacer fabrics finished with the IPM can be significantly improved. © 2013 Wiley Periodicals, Inc. J. Appl. Polym. Sci. 000: 000–000, 2013

KEYWORDS: microgels; coatings; composites; fibers; self-assembly

Received 12 December 2012; accepted 22 April 2013; Published online
DOI: 10.1002/app.39453

INTRODUCTION

Impact protective materials are used to protect the human body from injury or damage when subjected to impact, shock, vibration, or stab.[1] A usual way to make an impact protective material is to impregnate a substrate into a dilatant material, which remains soft until it is subjected to an impact, rendering it temporarily rigid due to the change of its characteristics. A dilatant material can return to its normal flexible state after the impact.[2,3]

One of the dilatant materials is the dilatant siloxane. It can be used on various substrates such as foams, fibers, non-woven materials, laminates, composites, knitted, or woven fabrics, functioning as an energy absorbing material in an active protection system or garment. Examples of applications include protective sportswear or pads for some dangerous sports such as horse riding, motorcycling, skiing, roller skating, skateboarding, etc.[3,4] Traditionally, dilatant siloxane materials are prepared from boron cross-linked organpolysiloxane due to their dilatant properties. In such dilatant materials, the entire organpolysiloxane chains are almost silanol-end-blocked or joined together by –OBO– linkages or both.[5,6] In some studies, a titanate ester is introduced into the traditional dilatant siloxane in order to improve its water-proof and washing fastness.[3] However, the coupling interaction originating from titanate ester can lead to the macroscopic cross-linking, and the dilatant property of impact protective material will fade away. Although traditional dilatant siloxane reveals significant improvement in impact protective performance, some drawbacks, such as high viscosity, higher reaction and dry temperatures still impede their further application and performance enhancement.

As silicone–boron copolymer impact protective materials are concerned, the molecular weight of copolymer is crucial to balance between impact protective performance and process difficulty. Although a higher molecular weight of copolymer can provide better impact protective performance, it will lead to the difficulty in transfer and process of product due to high viscosity of copolymer. In order to break the embarrassment situation, microgels containing heterogeneous cross-linking network, which are driven from the entanglements of polymer chains, would be an alternative. The idea is inspired by the theory of polymer coils[7] and microgel enhanced composite system[8,9] and has never been reported in synthesis of impact protective materials.

In this study, a new kind of impact protective material is proposed based on the concept of impact protective micro-gels (IPM) which was synthesized at a lower temperature. The

Applied Polymer SCIENCE

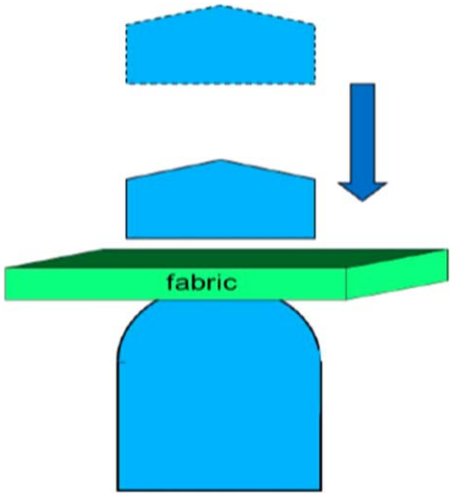

Figure 1. Schematic presentation of drop impact test. [Color figure can be viewed in the online issue, which is available at wileyonlinelibrary.com.]

silanol with good compatibility and organic boron were employed to prepare the linear silicone–boron composition. Both multi-functional chain extender agent and modification coupling agent were introduced to prepare the IPM. An analysis was carried out to examine the effect of the chain extender MDI on the performance and structure of the IPM, which was subsequently employed to finish a 3D spacer warp-knitted fabric to enhance its protective performance.

EXPERIMENTAL

Materials

The raw materials used included hydroxyl-end-blocked polydimethylsiloxane (HO-PDMS) (M_n = 2000), trimethoxyboroxine (TMOB; Aldrich, 95%), 4,4′-diphenylmethane diisocyanate (MDI), titanium isopropoxide (TIPT) and isopropyl alcohol (IPA, 98%; Aladdin, Shanghai, China). They all were used as received.

Synthesis of IPM

A typical procedure is described as follows. The precursor of HO-PDMS and TMOB with an appropriate weight ratio was firstly stirred at 90°C in an oil bath for 4 h. Then, MDI was added and the reaction was maintained for other 4 h to obtain an intermediate product. TIPT was then added to improve the washing fastness and reacted for other 16 h. The IPM was finally put on culture dishes and dried in an oven at 70°C for 72 h to obtain the final IPM product.

Finishing of 3D Spacer Fabric with IPM

3D spacer warp-knitted fabric was finished with the IPMs made with and without use of MDI via a conventional dip-coating method. The process included several steps. First, the IPM was dispersed into an isopropanol (IPA) solvent at an ambient temperature. The mixture was continuously stirred until a uniform dispersion was obtained. Then, the 3D fabrics were dip-coated with uniform dispersion and dried at 60°C for 4–8 hours.

Characterization

The analyses of complex viscosity, storage modulus, and loss modulus of the IPM samples obtained were performed at 25°C with a rheometer (AR 2000ex, TA Instruments) using a smart swap and measured from 0.1 to 400 rad/s. The structures of the IPM samples were analyzed by Fourier transform infrared (FT-IR) spectroscopy (Perkin Elmer System 2000 FT-IR) via the preparation of a KBr pellet. The morphology of the IPM samples, unfinished and finished 3D spacer fabrics were examined by using scanning electron microscopy (SEM; JEM-2000 operating at 15 kV, JEOL, Tokyo, Japan). The measurements of the particle size of microgels were conducted using a Brookhaven 90Plus particle size analyzer and the IPM for finished spacer fabrics were prepared by dispersing appropriate IPM into IPA.

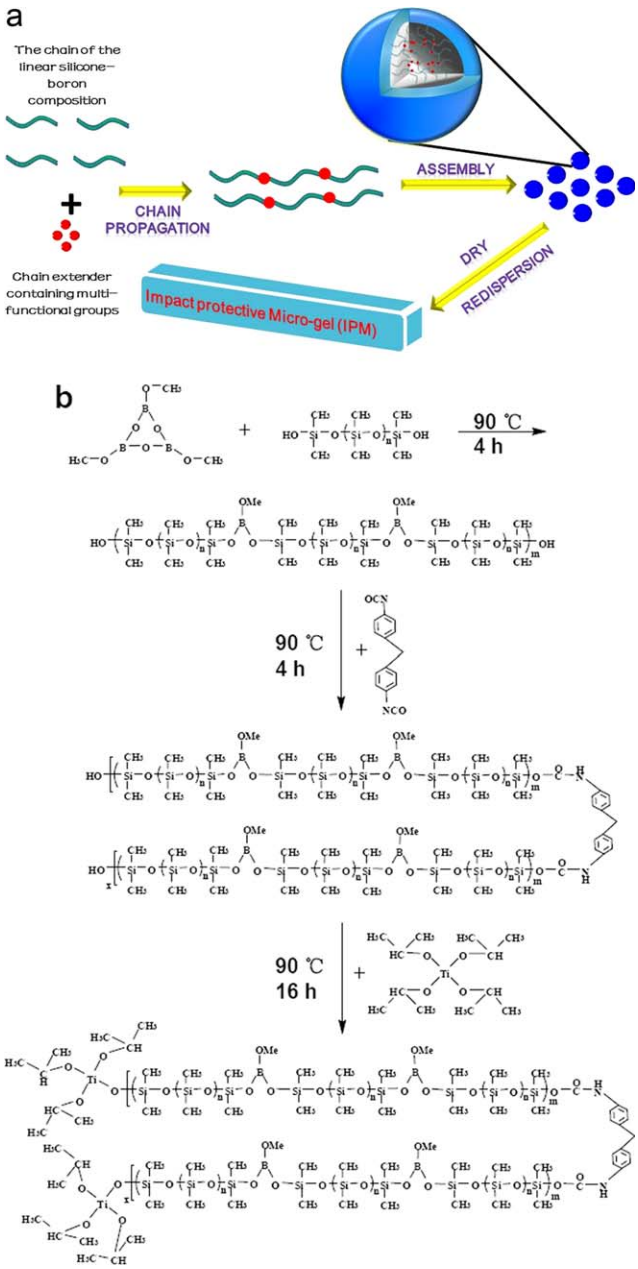

Figure 2. Schematic presentation of micro-gels formation. (a) The synthesis mechanism of IPM; (b) the chemical structure of reactants used and the reaction mechanism of IPM. [Color figure can be viewed in the online issue, which is available at wileyonlinelibrary.com.]

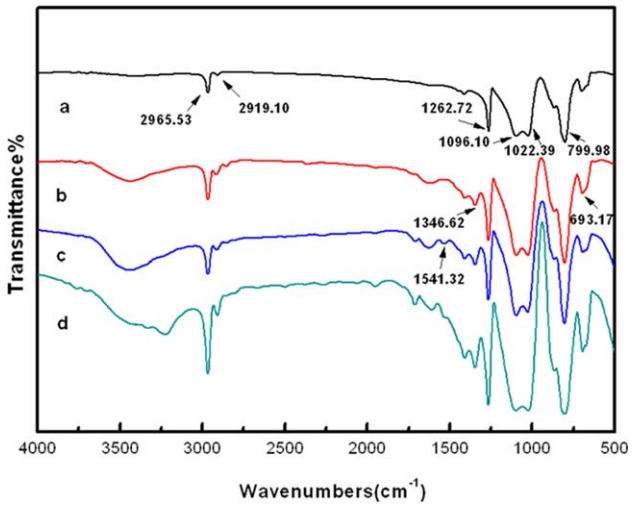

Figure 3. FTIR spectra of intermediate product and IPM [(a) native HO-PDMS; (b) copolymer of HO-PDMS and TMOB; (c) intermediate product with MDI; (d) IPM]. [Color figure can be viewed in the online issue, which is available at wileyonlinelibrary.com.]

The transmitted force was employed to characterize the impact protective performance of 3D spacer fabrics unfinished and finished with the IPM, and it was measured via a drop impact test as illustrated in Figure 1, in which a striker freely fell from a height of 1 m and impacted onto the upper surface of the fabric which was placed on a round support. The impact energy was 50 J. The size of the fabric was 12 cm × 10 cm. The transmitted force to the lower side of the fabric was recorded and employed to compare the impact protective performance of the 3D finished and unfinished spacer fabrics.

RESULTS AND DISCUSSION

Synthesis Mechanism of IPM

Although traditional dilatant materials reveal a significant improvement in impact protective performance, some drawbacks still exist. First, they should be synthesized and dried at higher temperatures (150–250°C) and toxic catalysts are frequently employed to decrease the reaction temperature and shorten the reaction time. The higher reaction and dry temperature not only raises the difficulty of the synthesis of materials, but also increases the consumption of energy. Moreover, the product is difficult to be transferred and processed due to higher viscosity. These drawbacks make continuous production difficult. On the other hand, when raw materials with lower molecular weight are employed to decrease the viscosity of products, their impact protective performance is unsatisfactory, because lower molecular weight of materials corresponds to poorer energy absorption efficiency of the polymer. In order to overcome these disadvantages, a new approach based on the formation of micro-gels was proposed to make IPM in this study. In Figure 2(**a**), the chains of the linear silicone–boron copolymer are further propagated by the introduction of chain extender MDI. When the length of polymer chains exceeds a critical length, the entanglements will start.[10,11] Hereafter, the polymer micro-gels will be self-assembled due to the entanglement of polymer chains. Meanwhile, the chemical structure of

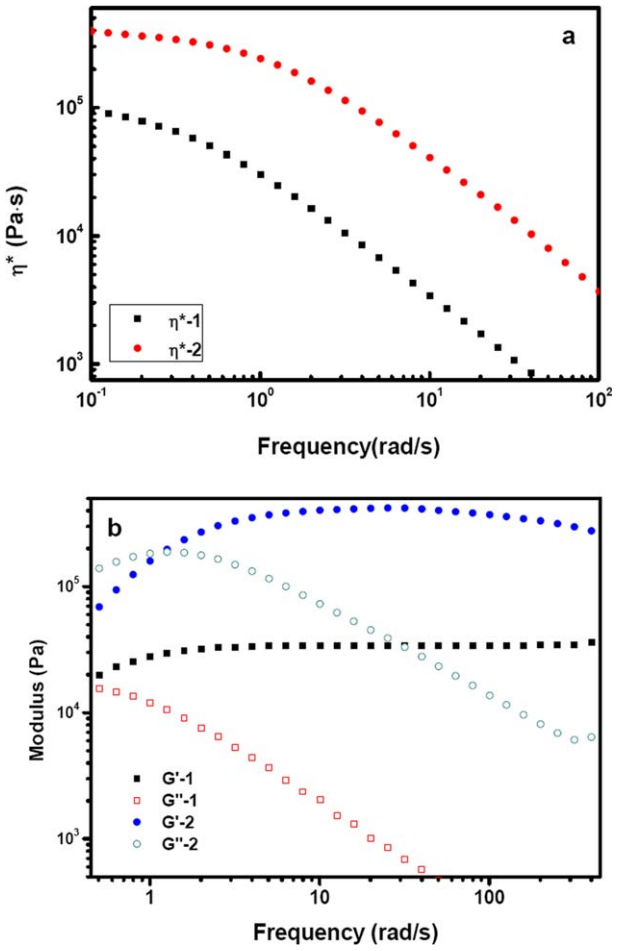

Figure 4. Rheological properties of IPM samples made with (sample 1) and without (sample 2) MDI: (a) complex viscosity; (b) storage modulus G' and loss modulus G''. [Color figure can be viewed in the online issue, which is available at wileyonlinelibrary.com.]

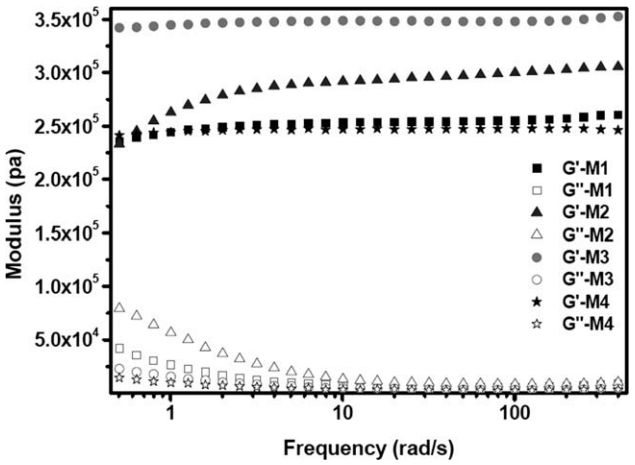

Figure 5. Evolution of storage modulus (G') and loss modulus (G'') of IPM samples made with various MDI levels. (The MDI contents are: M1, 1.5 wt %; M2, 2.0 wt %; M3, 2.5 wt %; M4, 3.0 wt %. The feeding ratio of PDMS to TMOB is 15 : 1 w/w, and the content of TIPT is fixed at 0.02 wt %.)

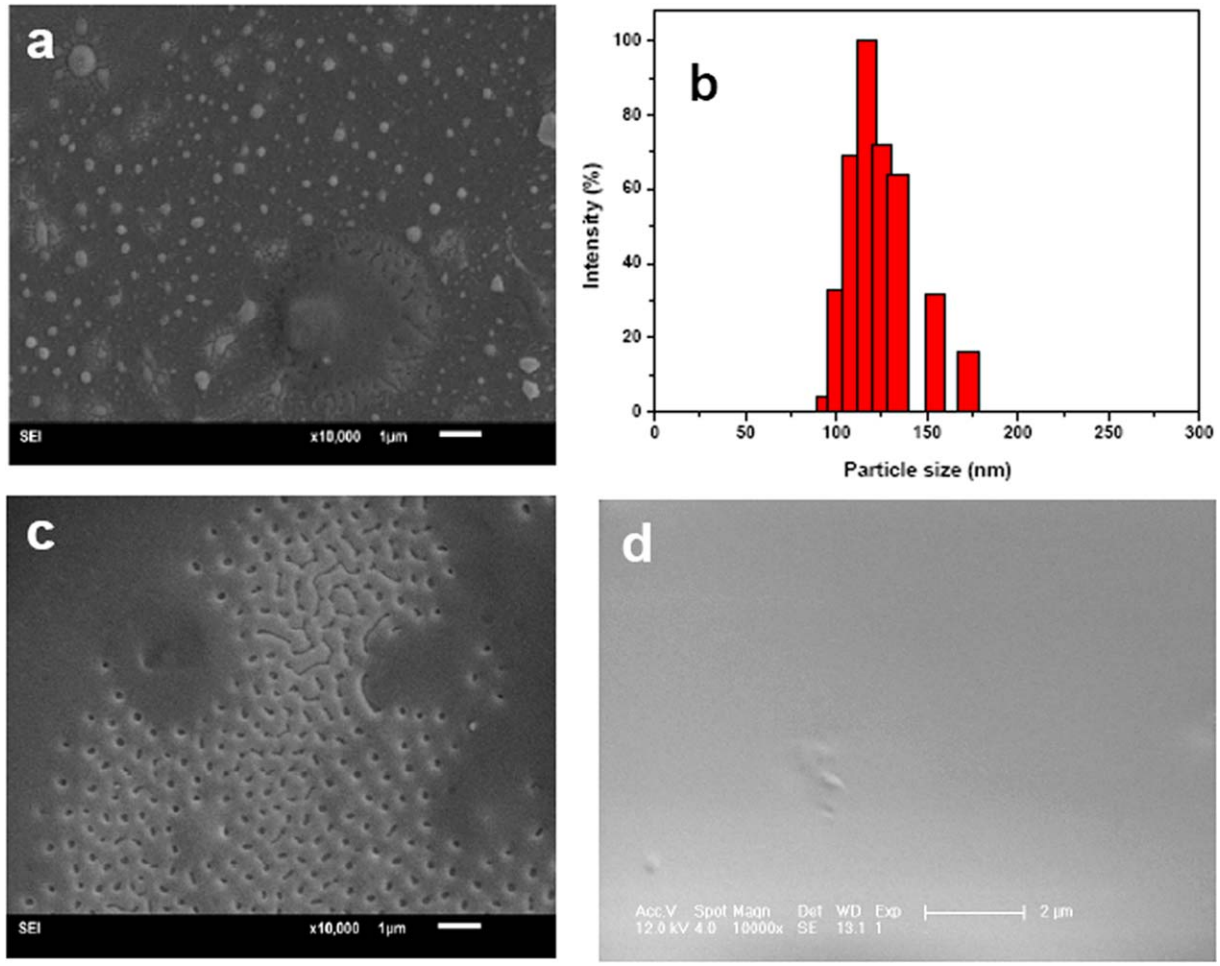

Figure 6. Evolution of sample morphology with various concentrations of IPM/IPA: (a) 0.3 wt %; (b) particle size and distribution of IPM; (c) 1.0 wt %, (d) 20 wt %. [Color figure can be viewed in the online issue, which is available at wileyonlinelibrary.com.]

reactants used and the reaction mechanism of IPM are also present in Figure 2(b).

Analysis of Fourier Transforms Spectra

Figure 3 shows the FT-IR transmittance spectra of the samples at different reaction stages. The native HO-PDMS (spectrum a) showing two peaks at 2965.53 and 2919.10 cm^{-1} is attributed to C–H bond in combination with CH_3 groups.[12] The bonds located at 1262.72 cm^{-1} mainly correspond to the Si–CH_3.[13–15] The bonds located at 1096.10, 1022.39, and 799.98 cm^{-1} are due to the asymmetric stretching of Si–O–Si.[16,17] In the copolymer of HO–PDMS and TMOB (spectrum b), the peak centered at 1346.62 cm^{-1} is due to B–O stretching.[16,18] The 693.17 cm^{-1} region is attributed to the Si–O–B bond.[19–21] It indicates that the covalent bonds are formed between the TMOB and the HO-PDMS. After the introduction of MDI (spectrum c), the peak at 1541.32 cm^{-1} is assigned to the CON–H, and the peak at 2270 cm^{-1} attributed to –N=C=O disappears. That implicates that the isocyanate group in MDI has reacted with the –OH, which responds to a higher molecular weight of the IPM. It should be noted that the characteristic bands of TIPT (spectrum d) at 1000 and 850 cm^{-1} are not present, which suggests that TIPT has already been reacted.[22]

Effect of Chain Extender MDI on Rheological Properties of IPM

MDI, as chain extender in the polymerization, can increase the molecular weight of polymer that leads to an increase in the viscosity of polymer.[23,24] In order to illustrate the role of MDI in the polymerization, the rheological properties of the IPM samples made with and without MDI were studied. In Figure 4(a), when the MDI is introduced, the complex viscosity is increased dramatically at the same frequency. This suggests that the introduction of the MDI can significantly increase the molecular weight of the polymer.[25] The storage modulus (G') and the loss modulus (G'') are also investigated and the results are shown in Figure 4(b). It can be found that while G' of the IPM sample made without MDI exhibits an obvious independence on the frequency, G' of the sample made with MDI increases with frequency, which implicates a impact hardening behavior. Meanwhile, G'' of the IPM sample made with MDI is much higher than that of the IPM sample made without MDI, which indicates that the sample with MDI can absorb more energy

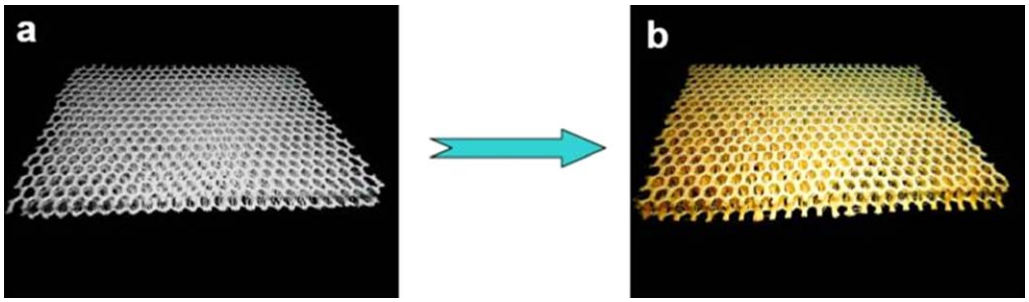

Figure 7. Photographs of 3D fabric before (a) and after (b) finishing. [Color figure can be viewed in the online issue, which is available at wileyonlinelibrary.com.]

than the sample without MDI when it suffers from impact. These results suggest that the addition of the MDI leads to the increase of G' and G'' because the MDI can increase the molecular weight of polymer. As aforementioned, the length of silicone–boron copolymer can propagate due to the chain extension reaction between MDI and hydroxyl terminated. When the length of polymer chains exceeds a critical length, the entanglements of polymer chains will occur and the macroscopic cross-linking network will form. Thus, the introduction of MDI can not only improves the module of IPM, but also endows impact hardening properties to the IPM sample due to the increment of molecular weight.

Effect of MDI Concentration on Rheological Properties of IPM

The effect of MDI concentration on rheological properties of IPM was also investigated in this study. The storage modulus (G') and the loss modulus (G'') were measured at 25°C from 0.1 to 400 rad/s for the IPM made with various MDI levels. In Figure 5, with the increment of MDI level, G' of the IPM samples exhibits different trends. As for M1 (MDI content is 1.5 wt %) and M2 (MDI content is 2.0 wt %), G' has a quick increase with frequency from 0.2 to 8.0 rad/s. After, G' increase trend decreases and gets very slow. This suggests that the IPM samples made with lower MDI contents own an impact hardening behavior. However, as for M3 (MDI content is 2.5 wt %) and M4 (MDI content is 3.0 wt %), G' is almost unchanged with the frequency, which suggests that the macroscopic cross-linking network is formed after the MDI content exceeds 2.5 wt %.[26–28] On the other hand, the G' level also changes with the MDI content. It increases when the MDI content increases from 1.5 wt % to 2.5 wt %. However, when the MDI content increases to 3.0 wt %, the G' level no longer increases. Inversely, it drops to the same level when the MDI content is 1.5 wt %. These results show that the MDI concentration significantly affects the mechanical performance of IPM samples due to the different cross-linking densities produced from the entanglement of polymer chains. At a lower level of MDI content, the shorter PDMS chains and the coupling interaction of TIPT induce a higher real cross-linking density. At a higher level of MDI content, the increment of the entanglement of polymer chains leads to a further increment of real cross-linking density, which causes a loss of dilatant behavior of the IPM samples. Only the IPM made with an appropriate level of MDI content can exhibit dilatant property because an appropriate real cross-linking density can induce the IPM structure transformation when the impact force is applied.

Morphology of IPM with Different Concentrations in IPA

In order to apply the IPM onto 3D spacer fabric, the IPM has to be dispersed in a solvent. In Figure 6(a), the IPM particles are well dispersed in IPA at a low concentration of 0.3%. The results of SEM and DLS in Figure 6(b) show that the particle size of IPM ranges from 150 to 170 nm. When the dispersed

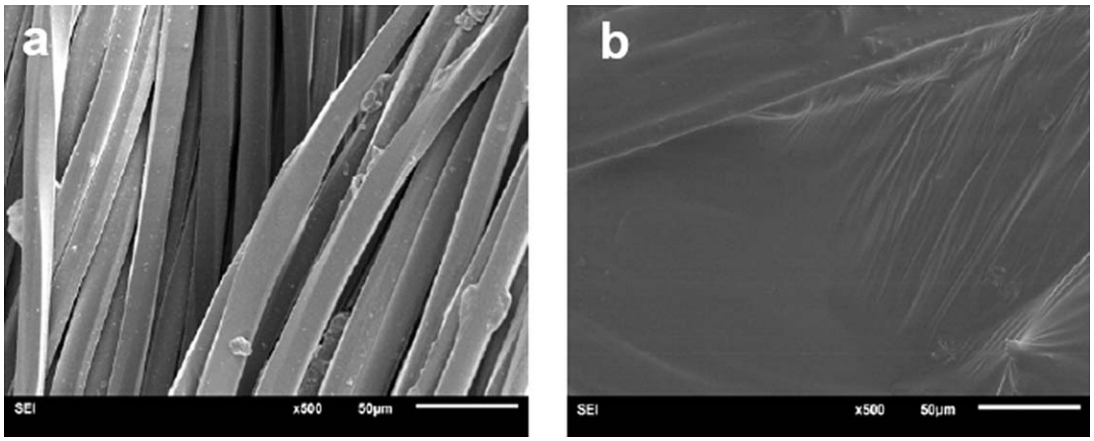

Figure 8. SEM images of 3D fabric surface before (a) and after (b) finishing with IPM.

Table I. Transmitted Force of 3D Spacer Fabric Before and After Finishing[a,b]

Fabric sample	Weight ratio between IPM and fabric	Transmitted force (kN)
Finished with IPM made without MDI	2.57	33.8
Finished with IPM made with MDI[c]	2.54	19.4
Control fabric	-	45.6

[a] The control fabric sample was prepared by sandwiching one 7 mm thickness unfinished fabric with two 5 mm thickness unfinished fabrics to prevent test value from exceeding the measurement scale of drop tester. To ensure the comparability of test results, the anti-impact protective fabrics were prepared by sandwiching one 7 mm thickness unfinished fabric with two 5 mm thickness finished fabrics.

[b] The height of the striker is 1.0 m.

[c] The MDI content of IPM made with MDI is 2.5 wt %.

solution concentration is increased up to 1.0% [Figure 6(c)], the partial IPM particles begins to gather and form a continuous state. When the dispersed solution concentration exceeds 20 wt %, the particles disappear and the morphology of IPM sample becomes a smooth, even and complete coat. Thus, if the IPM is used to dip-coat 3D spacer fabrics at this concentration, the surface of the finished fabrics will be covered with a smooth and even coat after drying, and no particles can be observed. On the other hand, the sample made without MDI exhibits entirely different morphology. No matter how the concentration of sample/IPA dispersion is, no particles can be found and the dispersion is completely transparent. Thus, it suggests that MDI is crucial to prepare nanoparticles and improve the impact protective performance of IPM.

Impact Protective Performance of 3D Spacer Fabrics Dip-Coated with IPM

3D spacer warp-knitted fabrics have been developed for impact protection.[29,30] In this study, 3D spacer warp-knitted fabric with hexagonal meshes was employed as substrate and dip-coated with the IPM to form the final impact protective product. The use of 3D mesh fabric structure can avoid the damage of the air permeability and flexibility of finished fabrics. Figure 7 shows the photographs of the 3D spacer fabric before and after finishing with the IPM. It can be seen that the color of the finished fabric is changed from the white to yellow.

Figure 8 shows the SEM images of the surface of 3D fabric before and after finishing with the IPM. Herein the MDI content in IPM made with MDI is 2.5 wt %. From Figure 8(b), it can be seen that the IPM is evenly distributed onto the 3D fabric surface with a complete coat.

The transmitted force is commonly employed to characterize the impact protective performance of an impact protective material. The lower the transferred force, the higher protective performance. Table I lists the results of transmitted force for 3D spacer fabric before and after finishing, tested with 50 J of impact energy. It can be seen that the 3D spacer fabric finished by the IPM made with 2.5 wt % MDI has the best impact protective performance because its transmitted force is the lowest one. The results suggest that the use of MDI during the synthesis of IPM can considerably improve the impact protective performance of IPM. Therefore, the IPM made with MDI can be used to finish 3D spacer fabric for making smart impact protective fabric for practical application.

CONCLUSIONS

IPM, which can be used as energy absorbing materials, was prepared via precipitation copolymerization of PDMS-OH and TMOB. And MDI was introduced as the chain extender to increase its molecular weight. The rheological properties and structural morphology of IPMs were analyzed. 3D warp-knitted spacer fabrics were dip-coated with IPMs made with and without use of MDI and their impact protective performance was assessed by measuring the transmitted force. According to the study, the following conclusions can be drawn:

(a) The micro-gels structure can be formed by the introduction of MDI during the synthesis process. The IPM with improved mechanical performance and impact hardening behavior can be achieved if an appropriate level of MDI content is adopted.
(b) The impact protective performance of 3D spacer fabrics finished with IPMs can be significantly improved, and 3D spacer fabric finished with IPM made of MDI has the lowest transmitted force, therefore, the best protective performance.

ACKNOWLEDGMENTS

This study was financially supported by the Innovation and Technology Commission of the Government of the Hong Kong Special Administrative Region of China (grant GHP/063/09TP) and the National Natural Science Foundation of China (grant 21004065) as well as the Program for New Century Excellent Talents in Universities of China.

REFERENCES

1. Harrigan, J. J.; Reid, S. R.; Peng, C. *Int. J. Impact Eng.* **1999**, *22*, 955.
2. Hiles, M. A. F.; Welwyn. US Pat. 4,346,205, **1982**.
3. Budden, G.; Francis, J. US Pat. Appl. 0305589, **2009**.
4. Dischler, L.; Moyer, T. T.; Henson, J. B. US Pat. Appl.5,776,839, **1998**.
5. Plant, D. J. US Pat. Appl. 7,608,314, **2009**.
6. Cauvin, S.; Liles, D.; Robson, S.; Stammer, A. US Pat. Appl.0039087, **2011**.
7. Flory, P. J. In Principles of Polymer Chemistry; Cornell University Press: Ithaca, NY, **1995**, p 519.
8. Hu, J.; Hiwatashi, K.; Kurokawa, T.; Liang, S. M.; Wu, Z. L.; Gong, J. P. *Macromolecules* **2011**, *44*, 7775.
9. Hu, J.; Hiwatashi, K.; Kurokawa, T.; Nakajima, T.; Wu, Z. L.;, Liang, S. M.; Gong, J. P. *Macromolecules* **2012**, *45*, 5218.

10. Ryu, J. H.; Chacko, R. T.; Bickerton, S.; Babu, R. P.; Thayumanavan, S. *J. Am. Chem. Soc.* **2010**, *132*, 17227.
11. Biagio, P. L. S.; Bulone, D.; Emannele, A.; Palma, M. U. *Biophys. J.* **1996**, *70*, 494.
12. Peña-Alonso, R.; Rubio, J.; Rubio, F.; Oteo, J. L. *J. Sol-Gel Sci. Technol.* **2002**, *25*, 255.
13. Bernas, A.; Peltopakka, B.; MÄki-Arvela, P.; Eränen, K.; Salmi, T.; Murzin, D. Y. *Res. Chem. Intermediates* **2007**, *33*, 645.
14. Orhan, J.-B.; Parashar, V.K.; Flueckiger, J.; Gijs, M. A. M. *Langmuir* **2008**, *24*, 9154.
15. Villegas, M. A.; Navarro, J. M. F. *J. Mater. Sci.* **1988**, *23*, 2464.
16. Beckett, M. A.; Rugen-Hankey, M. P.; Varma, S. K. *J. Sol-Gel Sci. Technol.* **2006**, *39*, 95.
17. Tsvetkova, I. N.; Shilova, O. A.; Shilov, V. V.; Shaulov, A. Y.; Gomza, Y. P.; Khashkovskii S. V. *Glass Phys. Chem.* **2006**, *32*, 218.
18. Wood, D. L.; Rabinovich, E. M. *Appl. Spectrosc.* **1989**, *43*, 263.
19. Kessler, V. G.; Spijksma, G. I.; Seisenbaeva, G. A.; Håkansson, S.;, Blank, D. H. A.;, Bouwmeester, H. J. M. *J. Sol-Gel Sci. Technol.* **2006**, *40*, 163.
20. Beckett, M. A.;, Rugen-Hankey, M. P.; Varma, K. S. *Chem. Commun.* **2001**, *6*, 1499.
21. Pola, J.; Herlin-Boime, N.; Brus, J.; Bastl, Z.; Vacek, K.; Šubrt, J.; Vorlíčekf, V. *Solid State Sci.* **2005**, *7*, 123.
22. Burgos, M.; Langlet, M. *Thin Solid Films* **1999**, *349*, 19.
23. Yeganeh, H.; Mehdizadeh, M. R. *Eur. Polym. J.* **2004**, *40*, 1233.
24. Tai, Z. X.; Yan, X. B.; Xue, Q. J. *J. Power Sources* **2012**, *213*, 350.
25. Treece, M. A.; Oberhauser, J. P. *Macromolecules* **2007**, *40*, 571.
26. Ramazani-Harandi, M. J.; Zohuriaan-Mehr, M. J.; Yousefi, A. A.; Ershad-Langroudi, A.; Kabiri, K. *Polym. Test.* **2006**, *25*, 470.
27. Geiser, V.; Leterrier, Y.; Manson, J. A. E. *Macromolecules* **2010**, *43*, 7705.
28. Chen, L.; Revel, S.; Morris, K.; Spiller, D. G.; Serpell, L. C.; Adams, D. J. *Chem. Commun.* **2010**, *46*, 6738.
29. Liu, Y. P.; Hu, H.; Long, H. R.; Zhao, L. *Textile Res. J.* **2012**, *82*, 773.
30. Liu, Y. P.; Hu, H.; Zhao, L.; Long, H. R. *Textile Res. J.* **2012**, *82*, 11.